Two Distinct Mechanisms for Regulation of Nonmuscle Myosin Assembly via the Heavy Chain: Phosphorylation for MIIB and Mts 1 Binding for MIIA[†]

Noriko Murakami,*[,‡] Leszek Kotula,[§] and Yu-Wen Hwang[||]

Laboratories of Neurobiochemistry, Molecular Neurobiology, and Molecular Regulations, New York State Institute for Basic Research in Developmental Disabilities, 1050 Forest Hill Road, Staten Island, New York 10314

Received February 15, 2000; Revised Manuscript Received June 9, 2000

ABSTRACT: In search of the regulation mechanisms for isoform specific myosin assembly, we have used the COOH-terminal fragments of nonmuscle myosin isoforms MIIA and MIIB (MIIA^{F46} and MIIB$^{\alpha F47}$) as a model system. Phosphorylation by protein kinase C (PK C) or casein kinase II (CK II) within or near the nonhelical tail-end domain inhibits assembly of MIIB$^{\alpha F47}$ [Murakami, N., et al. (1998) *Biochemistry 37*, 1989]. In the study presented here, we mutated the kinase sites to analyze the inhibition mechanisms of MIIB assembly by phosphorylation. Replacement of the CK II or PK C sites with Asp (MIIB$^{\alpha F47}$-CK-5D or -PK-4D) strongly inhibited the filament assembly, with or without Mg^{2+}, by significantly increasing the critical concentrations for assembly. Without Mg^{2+}, MIIB$^{\alpha F47}$-CK-5D or -PK-4D inhibited the assembly of wild-type (wt) MIIB$^{\alpha F47}$ by either mixing as homofragments or forming heterofragments. With 2.5 mM Mg^{2+}, MIIB$^{\alpha F47}$-wt promoted assembly of MIIB$^{\alpha F47}$-CK-5D and -PK-4D in homofragment mixtures, but not by forming heterofragments. MIIA^{F46} coassembled with MIIB$^{\alpha F47}$-wt and -CK-5D and altered their assembly patterns. In contrast, assembly of MIIB$^{\alpha F47}$-PK-4D was unchanged by MIIA^{F46}. A metastasis-associated protein, mts 1, bound in a Ca^{2+}-dependent manner to MIIA^{F46}, but not appreciably to MIIB$^{\alpha F47}$. At 0.15 M NaCl, mts 1-Ca^{2+} not only inhibited MIIA^{F46} assembly but also disassembled the MIIA^{F46} filaments. Mts 1, however, did not affect the assembly of MIIB$^{\alpha F47}$ in MIIA^{F46} and MIIB$^{\alpha F47}$ mixtures, indicating that mts 1 is an inhibitor specific to MIIA assembly. Our results suggest strongly that assembly of MIIA and MIIB is regulated by distinct mechanisms via tail-end domains: phosphorylation of MIIB and mts 1 binding to MIIA. These mechanisms may also function to form MIIA or MIIB homofilaments by selectively inhibiting MIIB or MIIA assembly.

Higher vertebrates have at least two genes for nonmuscle myosin II heavy chains, type A (MIIA) and type B (MIIB) isoforms (*1*, *2*). These myosins have been shown to distribute within moving cells in isoform specific patterns (*3*−*6*). Because MIIA and MIIB have distinct enzymic activities and F-actin sliding speeds (*5*), it is reasonable to believe that MIIA and MIIB have different roles in cell motility. Nonmuscle myosins form cofilaments even with muscle myosins in vitro (*7*, *8*). Cells, therefore, must have mechanisms for assembling myosins in an isoform specific manner. Amino acid sequences within the α-helical coiled-coil domains are well-conserved between MIIA and MIIB. In contrast, the nonhelical tail-end domains have the sequences specific to each isoform, which can be phosphorylated by casein kinase II (CK II)[1] and protein kinase C (PK C) (*9*). Although it is well-accepted that filament formation of vertebrate smooth muscle and nonmuscle myosins is regulated by phosphorylation of the regulatory light chains, these myosins appear to share the same regulatory light chains (*10*, *11*). Therefore, light-chain phosphorylation cannot be the mechanism for isoform specific filament formation. Because the nonhelical tail-end domains are known to influence myosin assembly (*12*−*14*), we have hypothesized that phosphorylation of the tail-end region plays a role in regulation of isoform specific assembly of nonmuscle myosin II molecules. In a previous study, we reported two closely related forms of MIIB expressed in rabbit brains, designated MIIB$^{\alpha}$ and MIIB$^{\beta}$ (*9*). PK C phosphorylated the 47 kDa COOH-terminal fragment of MIIB$^{\alpha}$ and MIIB$^{\beta}$ (MIIB$^{\alpha F47}$ and MIIB$^{\beta F47}$) at one and two positions, respectively, within multiple sites clustered near the predicted junction of the α-helical and nonhelical domains. The phosphorylation inhibits assembly of MIIB$^{\alpha F47}$ and MIIB$^{\beta F47}$. Although PK C phosphorylates human MIIA at a single site near the end of the α-helical domain (*15*, *16*), it has no detectable effect on assembly of the MIIA fragments (MIIA^{F46}) (*9*). CK II phosphorylates at five and four potential sites within the

[†] This work was supported by the New York State Office of Mental Retardation and Developmental Disabilities.

* Corresponding author. Phone: (718) 494-5324. Fax: (718) 698-7916. E-mail: pjisadog@interport.net.

[‡] Laboratory of Neurobiochemistry.

[§] Laboratory of Molecular Neurobiology.

[||] Laboratory of Molecular Regulations.

[1] Abbreviations: MIIA^{F46}, COOH-terminal 46 kDa fragments of nonmuscle myosin isoform MIIA; MIIB$^{\alpha F47}$, COOH-terminal 47 kDa fragments of nonmuscle myosin isoform MIIB$^{\alpha}$; mts 1, metastasis-associated protein; PK C, protein kinase C; CK II, casein kinase type II; PK-5A, five PK C sites mutated to Ala; PK-2D, PK C sites mutated to Asp and Ala at two and three positions, respectively; PK-2E, same sites as PK-2D mutated but to Glu; PK-3E, PK C sites mutated to Glu and Ala at three and two positions; PK-4D, PK C sites mutated to Asp and Ala at four and one positions; CK-5A or CK-5D, five CK II sites mutated to Ala or Asp, respectively.

10.1021/bi000347e CCC: $19.00
Published on Web 08/23/2000

Table 1: Summary of the Mutants Used for in Vitro and in Vivo Studies

mutant	amino acid residues changed	
	PK C site	CK II site
MIIB$^{\alpha F47}$-wt	SFSSSRS	SLELSDDDTESKTSDVNETQPPQSE
MIIB$^{\alpha F47}$-PK-5A	AFAAARA	
MIIB$^{\alpha F47}$-PK-2D	AFAADRD	
MIIB$^{\alpha F47}$-PK-2E	AFAAERE	
MIIB$^{\alpha F47}$-PK-3E	EFAAERE	
MIIB$^{\alpha F47}$-PK-4D	DFDADRD	
MIIB$^{\alpha F47}$-CK-5A		ALELADDDAESKTADVNETQPPQAE
MIIB$^{\alpha F47}$-CK-5D		DLELDDDDDESKTDDVNETQPPQDE

nonhelical tail-end domain of MIIB$^{\alpha F47}$ and MIIB$^{\beta F47}$, respectively. An average of two of the four sites are phosphorylated in MIIB$^{\beta F47}$, whereas all five sites can be fully phosphorylated by CK II in MIIB$^{\alpha F47}$. MIIA^{F46} has a single CK II site within the corresponding domain. These phosphorylation levels parallel the effects of phosphorylation on filament assembly: CK II strongly inhibits MIIB$^{\alpha F47}$ and slightly inhibits MIIB$^{\beta F47}$, but it does not detectably affect MIIA^{F46} assembly. However, it has not been addressed whether phosphorylation of heavy chains by these kinases plays a role for homofilament formation in mixtures of MIIA and MIIB.

A metastasis-associated 9−10 kDa protein, mts 1, belongs to the S100 subfamily of calcium binding proteins and is also called pEL98, 18A2, 42A, p9Ka, calvasculin, S100A4, FSP1, or CAPL. Although mts 1 is expressed in most normal tissues (*17*), high concentrations of mts 1 are expressed in metastatic tumor cells (*18*) and also in highly motile normal cells such as activated macrophages (*19*). In addition, transfection of nonmetastatic tumor cells with the mts 1 gene promotes cell metastasis (*20*, *21*). Mts 1 binds to nonmuscle myosin heavy chains MIIA and MIIB (*22*, *23*). The binding to MIIA (platelet myosin) causes destabilization of the myosin filaments (*22*). A recent study by Kriajevska et al. (*23*) has shown that mts 1 binds at the tail end of MIIA and inhibits the phosphorylation of MIIA by PK C. Because the PK C phosphorylation sites differ between MIIA and MIIB (*9*), mts 1 could bind to MIIA and MIIB differently. This study was carried out (1) to establish the inhibition mechanism of MIIB assembly by phosphorylation, (2) to test the effect of MIIB phosphorylation on homofilament assembly in the MIIA and MIIB mixtures, and (3) to determine the binding specificity and functions of mts 1 between MIIA and MIIB. We show that there are two distinct mechanisms for inhibiting nonmuscle myosin assembly via the tail-end region: phosphorylation of MIIB and mts 1 binding to MIIA.

MATERIALS AND METHODS

Materials. DNA polymerase, restriction enzymes, and a DNA ladder standard were purchased from NewEngland Bio Labs (Beverly, MA); M15[pREP4] and Ni−NTA resin were from Qiagen (Valencia, CA). Other analytical chemicals were obtained from Sigma (St. Louis, MO).

Mutation of MIIB$^{\alpha F47}$ at the PK C or CK II Sites. Five types of mutation were carried out at five PK C sites (see Table 1). Primers (sense strand) for these mutations were 5′-CGTGGGGGCCCAATTGCATTCGCTGCCGCTCGAGCTGGCCGGCGCCAGCTGCAC-3′ (PK-5A), 5′-CGTGGGGGCCCAATTGCATTCGCTGCCGACCGAGATGGCCGGCGCCAGCTGCAC-3′ (PK-2D), 5′-GTGGGGGCCCAATTGCATTCGCTGCCGAGCGAGAAGGCCGGCGCCAGCTG-3′ (PK-2E), 5′-GTGGGGGCCCAATTGAATTCGCTGCCGAGCGAGAAGGCCGGCGCCAGCTG-3′ (PK-3E), and 5′-CGTGGGGGCCCAATTGACTTCGATGCCGACCGAGATGGCCGGCGCCAGCTGCAC-3′ (PK-4D). These were used for PCR with an antisense primer (Myo-3′, 5′-CTTCTCTAGACTTCATTCGGACTGGG-3′). The reaction mixtures for the first PCR contained 4 μg of the sense primer, 2 μg of the antisense primer, 2% DMSO, 4 units of vent polymerase, 0.25 mM dNTPs, 2 mM $MgCl_2$, 10 mM KCl, 10 mM $(NH_4)_2SO_4$, 20 mM Tris-HCl (pH 8.8), and 0.1% Triton X-100 in a final volume of 100 μL. The MIIB$^{\alpha F47}$ expression vector (pND-MIIB$^{\alpha F47}$, 0.5 μg) (*9*) was used as a template. The PCR was carried out at 94 °C for 4 min once; 92 °C for 30 s and 68 °C for 1 min for five cycles; 92 °C for 1 min, 55 °C for 1 min, and 72 °C for 30 s for 25 cycles; and then 55 °C for 30 s, 72 °C for 5 min, and 25 °C for 15 min once. For mutation of CK II sites, two primers (5′-sense and 3′-antisense), 66mers each having completely matched overlaps of 20 bases were synthesized for each set of mutations. For mutation of the five CK II sites to Asp (CK-5D), a 5′-sense primer was prepared as 5′-CTGCACATCGAG*GGCGCC*GACCTGGAGCTGGATGATGACGACGATGAAAGTAAGACCGATGATGTC-3′, and the 3′-antisense primer was 5′-CTTCTCTAGACTTCATTCGTCCTGGGGTGGCTGCGTCTCGTTGACATCATCGGTCTTACTTTCATC-3′. Similarly, for mutation of all CK II sites to Ala (CK-5A), the 5′-sense primer was 5′-CTGCACATCGAG*GGCGCC*GCCCTGGAGCTGGCCGATGACGACGCAGAAAGTAAGACCGCAGATGTC-3′, and the 3′-antisense primer was 5′-CTTCTCTAGACTTCATTCGGCCTGGGGTGGCTGCGTCTCGTTGACATCTGCGGTCTTACTTTCTGC-3′. The *italic* region is the newly created *Nar*I site to quickly test the mutation. Two 66mers (4 μg each) for each set were extended into 112 bp DNAs by PCR in the reaction mixtures described above. The reaction was carried out at 94 °C for 2 min once; 92 °C for 1 min, 60 °C for 1 min, and 72 °C for 20 s for 25 cycles; and then 72 °C for 5 min and 25 °C for 15 min once. All PCR products were applied to Visigel (Stratagene, La Jolla, CA), and the 156 or 112 bp DNA bands for the PK C or CK II site mutations, respectively, were cut out. The gel slices were then put into dialysis tubing containing 0.3 mL of Tris-acetate EDTA buffer, and the DNAs were electroeluted at 100 V for 20 min followed by EtOH precipitation. Second PCR was carried out by using PCR products and a 5′-end sense DNA oligomer (1 μg) (Myo-5′, 5′-GATCCTGTACAAGGCCCAGTTCGAGCG-3′ containing a *Bsr*GI restriction site) as primers in the presence of 8 mM $MgCl_2$, 3% DMSO, and other components as described for the first PCR at 94 °C for 4 min once; 92 °C for 1 min and

68 °C for 2 min for five cycles; 92 °C for 60 s, 65 °C for 90 s, and 72 °C for 75 s for 25 cycles; and then 65 °C for 30 s, 72 °C for 5 min, and 25 °C for 15 min. The 1.2 kb DNAs from agarose gels were purified by using Wizard PCR Preps DNA Purification Resin (Promega, Madison, WI). (See Table 1 for a summary of various mutations.)

Expression of Recombinant Proteins in E. coli. cDNAs encoding MIIB$^{\alpha F47}$ with and without mutations at various sites were ligated into pND between *Bsr*GI and *Xba*I sites. Expression and purification of the mutant proteins in and from *E. coli* were performed by the methods described previously (*9*, *16*). An expression vector (pGE-30) containing a full-length mts 1 cDNA with a polyhistidine tag was a gift from M. Kriajevska (Danish Cancer Society, Copenhagen, Denmark). Mts 1 was purified from the M15[pREP4] cells transformed with the expression vector, according to the methods given by M. Kriajevska (personal communication) with a minor modification. In brief, bacterial pellets obtained from 250 mL of cultures were suspended in 12 mL of sonication buffer containing 50 mM Tris-HCl, 10 mM imidazole-HCl, and 0.2 M NaCl at pH 7.5, with protease inhibitors [0.1 mM PMSF and leupeptin, pepstatin A, and aprotinin (5 μg/mL each)], and were pulse-sonicated (*16*). After centrifugation at 27000*g* for 30 min, the NaCl concentration of the supernatant was adjusted to 1 M before mixing with Ni−NTA resin (3 mL as a 50% slurry) equilibrated with sonication buffer. The lysate/resin mixtures were incubated for 60 min at 4 °C with gentle shaking, transferred to a small column, and washed with 1 M NaCl, 50 mM Tris-HCl, and 10 mM imidazole-HCl at pH 7.5. The resin-bound protein, eluted with 1 M NaCl and 0.1 M sodium acetate at pH 4.0 (buffer A), was dialyzed against 10 mM MES (pH 6.2), 50 mM NaCl, 0.5 mM EDTA, and 1 mM DTT, and kept at −70 °C until use. Protein concentrations were determined by the method of Lowry et al. (*24*), using BSA as a standard.

Mts 1−Heavy Chain Binding Assay. Heavy chain fragments and mts 1 at various molar ratios were incubated for 30 min at 4 °C in 10 mM imidazole-HCl (pH 7.5) and 0.1 mM DTT (buffer B), including 0.2 M NaCl with or without 0.1 mM Ca^{2+} in a final volume of 0.3 mL at 0.3 mg of fragment/mL (3.2−3.3 μM fragments or 6.4−6.6 μM peptides). The Ca^{2+} concentration was adjusted by adding 10 mM $CaCl_2$. The mixtures were then transferred to microcentrifuge tubes containing Ni−NTA resin (50 μL of slurry) equilibrated with buffer B containing 0.2 M NaCl and were incubated overnight. The tubes were microcentifuged at 10000*g* for 5 min, and the resin was washed twice by centrifugation using the same buffer with or without Ca^{2+}. The resin-bound proteins were eluted with 100 μL of buffer A. Each eluate (50 μL) was mixed with water (50 μL) and a SDS sample buffer (100 μL) and subjected to SDS−PAGE using a Tris-tricine buffer system (*25*).

Filament Assembly. Heavy chain fragments were incubated at 4 °C overnight in the presence of 10 mM imidazole-HCl (pH 7.5), 0.1 mM EGTA, and various concentrations of NaCl with 1 mM EDTA or 2.5 mM Mg^{2+}. After microcentrifugation at 13600*g* for 30 min, the amounts of protein recovered in the supernatants were determined by the modified Bradford method (*9*) with MIIB$^{\alpha F47}$ as a standard (*9*). The percent recovery of protein in the supernatants was calculated by taking the amount of protein, for each point, measured before centrifugation, as 100%. An aliquot of each sample was also subjected to SDS−PAGE (*26*).

To test the effect of mts 1 on myosin assembly, a total of 30 μg of MIIA^{F46}, MIIB$^{\alpha F47}$, or the MIIA^{F46}/MIIB$^{\alpha F47}$ mixture [in 0.6 M NaCl, 10 mM imidazole-HCl (pH 7.5), 0.1 mM DTT, 1 mM EDTA, and 0.1 mM EGTA (buffer C)] was incubated with mts 1 at various molar ratios, in the presence of Mg^{2+} with or without Ca^{2+}. The final concentrations were adjusted to 0.1, 0.15, or 0.2 M NaCl, 2.5 mM Mg^{2+}, and 0.1 mM Ca^{2+} by using 1 M NaCl and buffer B, in a final volume of 0.1 mL. After incubation overnight, the mixtures were ultracentrifuged (Beckman TL-100) at 279000*g* for 20 min. The resultant supernatants were removed, and the precipitates, where indicated, were suspended in 50 μL of 0.2 M NaCl. An aliquot of these fractions was subjected to SDS−PAGE (*25*, *26*) to measure the amounts of heavy chain fragments as described previously (*27*).

Effects of Mts 1 on MIIA^{F46} Filaments. MIIA^{F46} filaments were prepared by reducing the NaCl concentrations of the heavy chain preparations to either 50 or 150 mM with buffer B in the presence of 2.5 mM Mg^{2+} and 0.1 mM Ca^{2+}. Various amounts of mts 1 in 50 μL of the corresponding salt solutions were mixed with 100 μL of the filament solutions (30 μg). Where indicated, 0.1 mM EGTA was added instead of Ca^{2+}. After incubation at 4 °C for 1 h, the mixtures were ultracentrifuged as described above, and the amounts of MIIA^{F46} in the supernatants were measured as described in ref *27* from the Coomassie blue-stained gels (*26*).

Other Methods. DNA sequencing of the mutant MIIBs$^{\alpha F47}$ was carried out with an automated fluorescent DNA sequencer (AnaGen, Palo Alto, CA).

RESULTS

Effects of Mutations on Filament Assembly. (1) Effect of NaCl Concentrations. Filament-forming properties of the MIIB^{F47} mutants were measured first in the presence of various concentrations of NaCl with either 1 mM EDTA or 2.5 mM Mg^{2+}. With EDTA, more than 60% of MIIB$^{\alpha F47}$-wt was recovered in the supernatant fractions at both 50 and 250 mM NaCl. At intermediate salt concentrations, practically all of the fragments sedimented (Figure 1A). Mutation of the five CK II sites to Ala (CK-5A) did not significantly alter the properties of MIIB$^{\alpha F47}$, except at 50 mM, where almost all of the MIIB$^{\alpha F47}$-CK-5A sedimented (Figure 1A). In the parallel assay, mutation to Asp at the five CK II sites (CK-5D) strongly inhibited MIIB assembly; approximately 60% of the MIIB$^{\alpha F47}$-CK-5D was recovered in the supernatant at 50 mM NaCl, and almost all of the fragments were found in the supernatant at NaCl concentrations of >100 mM. This assembly pattern was very similar to that of the MIIB$^{\alpha F47}$ phosphorylated by CK II in vitro (*9*). Mutation of the five PK C sites to Ala (PK-5A) did not alter the filament-forming properties of MIIB$^{\alpha F47}$ at the salt concentration range that was used. Assembly of MIIB$^{\alpha F47}$-PK-2D (A-F-A-A-**D**-R-**D**, to mimic 1 mol of phosphate incorporated/mol of peptide) was more susceptible to NaCl than to the wild type, at a concentration of 0.175 M and higher as well as lower than 0.1 M (Figure 1A). However, between 0.1 and 0.15 M NaCl, this mutant sedimented to an extent similar to that of

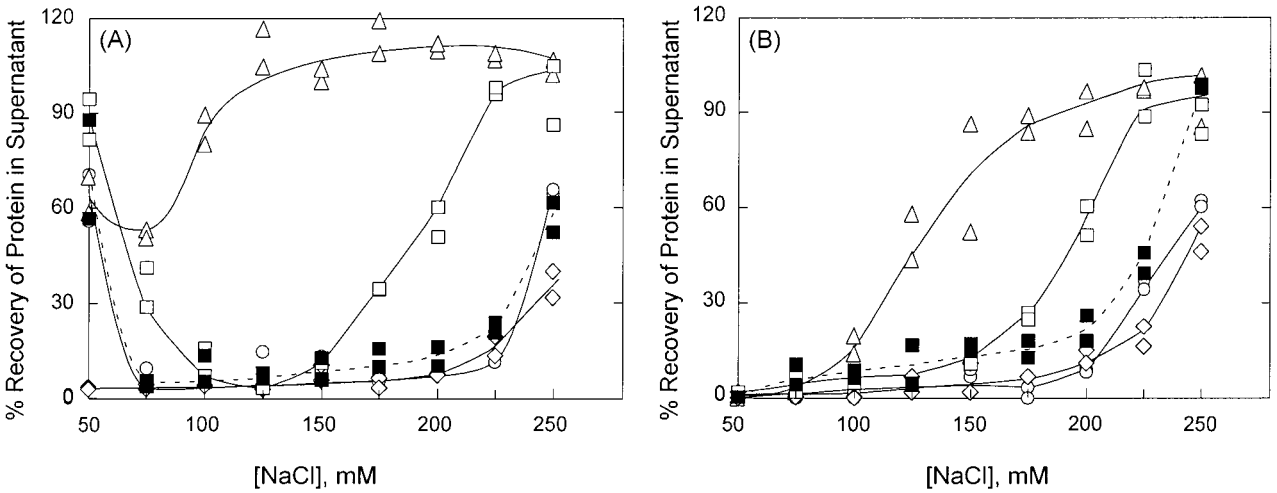

FIGURE 1: Assembly properties of MIIB$^{\alpha F47}$ and its mutants at various salt concentrations. The percent recovery of the fragments in the supernatant is shown. Fragments (0.1 mg/mL) were incubated in the presence of various concentrations of NaCl without (A) or with (B) 2.5 mM Mg^{2+} in a final volume of 0.3 mL, as described in Materials and Methods. The amount of proteins recovered in the supernatant after centrifugation was determined as described previously (*9*): (○) MIIB$^{\alpha F47}$-wt, (△) MIIB$^{\alpha F47}$-CK-5D, (◇) MIIB$^{\alpha F47}$-CK-5A, (□) MIIB$^{\alpha F47}$-PK-2D, and (■) MIIB$^{\alpha F47}$-PK-5A.

MIIB$^{\alpha F47}$-wt. Addition of 2.5 mM Mg^{2+} to the reaction mixtures significantly reduced protein recovery rates in the supernatant at low salt concentrations; at <0.1 M NaCl, most of the fragments sedimented via microcentrifugation, regardless of the types of mutation (Figure 1B). At >0.1 M NaCl, Mg^{2+} did not appear to affect the assembly of MIIB$^{\alpha F47}$-wt, -PK-2D, -PK-5A, or -CK-5A. However, it clearly enhanced the assembly of MIIB$^{\alpha F47}$-CK-5D between 0.1 and 0.175 M NaCl. Mutation to Glu at the same sites as PK-2D (MIIB$^{\alpha F47}$-PK-2E) altered the assembly patterns very similar to those of PK-2D with or without Mg^{2+} (not shown).

(2) Critical Concentrations. The critical concentrations for assembly of the various mutants were determined at 0.15 M NaCl. Without Mg^{2+}, MIIB$^{\alpha F47}$-wt formed filaments at concentrations as low as 2 μg/mL (0.04 μM heavy chain peptides or 0.02 μM heavy chain fragments), and the amounts recovered in the supernatant were at a constant level at all protein concentrations (Figure 2a). Under the same conditions, all of the MIIB$^{\alpha F47}$-CK-5D added to the reaction mixtures was recovered in the supernatant. MIIB$^{\alpha F47}$-PK-2D formed filaments at concentrations of >20 μg/mL, causing protein recoveries to plateau (Figure 2a); a critical concentration for assembly of MIIB$^{\alpha F47}$-PK-2D calculated from the figure was 15 μg/mL (0.16 μM fragments). MIIB$^{\alpha F47}$-PK-2E gave values very similar to those of PK-2D. Thus, replacement of the PK C sites with Asp appeared to have the same effects as those with Glu on MIIB$^{\alpha F47}$ assembly. Mutation of MIIB$^{\alpha F47}$ to CK-5A or PK-5A did not change the critical assembly concentrations from those of wt (see Table 2 for a summary). Mg^{2+} at 2.5 mM, basically, did not alter the critical concentrations for assembly of wt and PK-2D (Figure 2b) as well as PK-2E. Because MIIB$^{\alpha F47}$-CK-5D did not assemble at concentrations of <80 μg/mL (Figure 2b), the analysis was repeated by using higher concentrations of the fragments (Figure 2c). In the presence of Mg^{2+}, MIIB$^{\alpha F47}$-CK-5D assembled at concentrations of 0.3 mg/mL and the protein recovery in the supernatant remained at this plateau level; a critical concentration calculated from this experiment was 0.25 mg/mL (2.7 μM fragments). Without Mg^{2+}, more than 90% of the MIIB$^{\alpha F47}$-CK-5D added to the reaction mixtures was recovered in the supernatants, even at a concentration of 1 mg/mL. Again, almost all of the MIIB$^{\alpha F47}$-PK-2D sedimented under similar conditions.

The assembly properties of MIIB$^{\alpha F47}$-PK-2D or -PK-2E (Figure 1) show that replacement of Ser with acidic amino acids at two positions does not fully mimic the effect of phosphorylation by PK C. Therefore, we mutated additional positions; a total of three and four PK C sites were altered to Glu (PK-3E, E-F-A-A-E-R-E) and Asp (PK-4D, D-F-D-A-D-R-D), respectively. The critical concentrations of PK-3E and PK-4D, without Mg^{2+}, were calculated as 0.09 and ≥0.3 mg/mL, respectively. Mg^{2+} (2.5 mM) decreased these values to 0.05 and 0.15 mg/mL (0.53 and 1.6 μM fragments) for PK-3E (not shown) and PK-4D (Figure 2d), respectively. The assembly characteristics of MIIB$^{\alpha F47}$-PK-4D, tested at various salt concentrations, were very similar to those of the MIIB$^{\alpha F47}$ phosphorylated by PK C in vitro, reported previously (*9*). Thus, the extent of inhibition of assembly clearly depended upon the number of acidic amino acids inserted at the PK C sites. Two negative charges created by COO^- were not enough to mimic the effect of PO_4^{2-} on MIIB$^{\alpha F47}$ assembly.

Effects of MIIB-wt on Assembly of the Asp Mutants. Next, we attempted to address how coexistence of the phosphorylated and unphosphorylated forms of MIIB affects each other's assembly. For this purpose, two sets of experiments were carried out by using (1) heterofragments formed with a 1:1 ratio of MIIB$^{\alpha F47}$-wt and -CK-5D (named W/CK-D) and (2) mixtures of homofragments MIIB$^{\alpha F47}$-wt and -CK-5D (W_2 + CK-D_2), in a 1:1 ratio. Statistically, 50% of the proteins should form heterofragments when equal amounts of MIIB$^{\alpha F47}$-wt and -CK-5D are denatured and renatured. This preparation is regarded as heterofragments. In the presence of EDTA, MIIB$^{\alpha F47}$-CK-5D, homofragment mixtures (W_2 + CK-D_2), and heterofragments (W/CK-D), none of the three preparations sedimented at all, at the protein concentrations that were used (Figure 2e). The denaturing and renaturing procedures used for W/CK-D did not alter the rate of assembly of MIIB$^{\alpha F47}$-wt (Figure 2e).

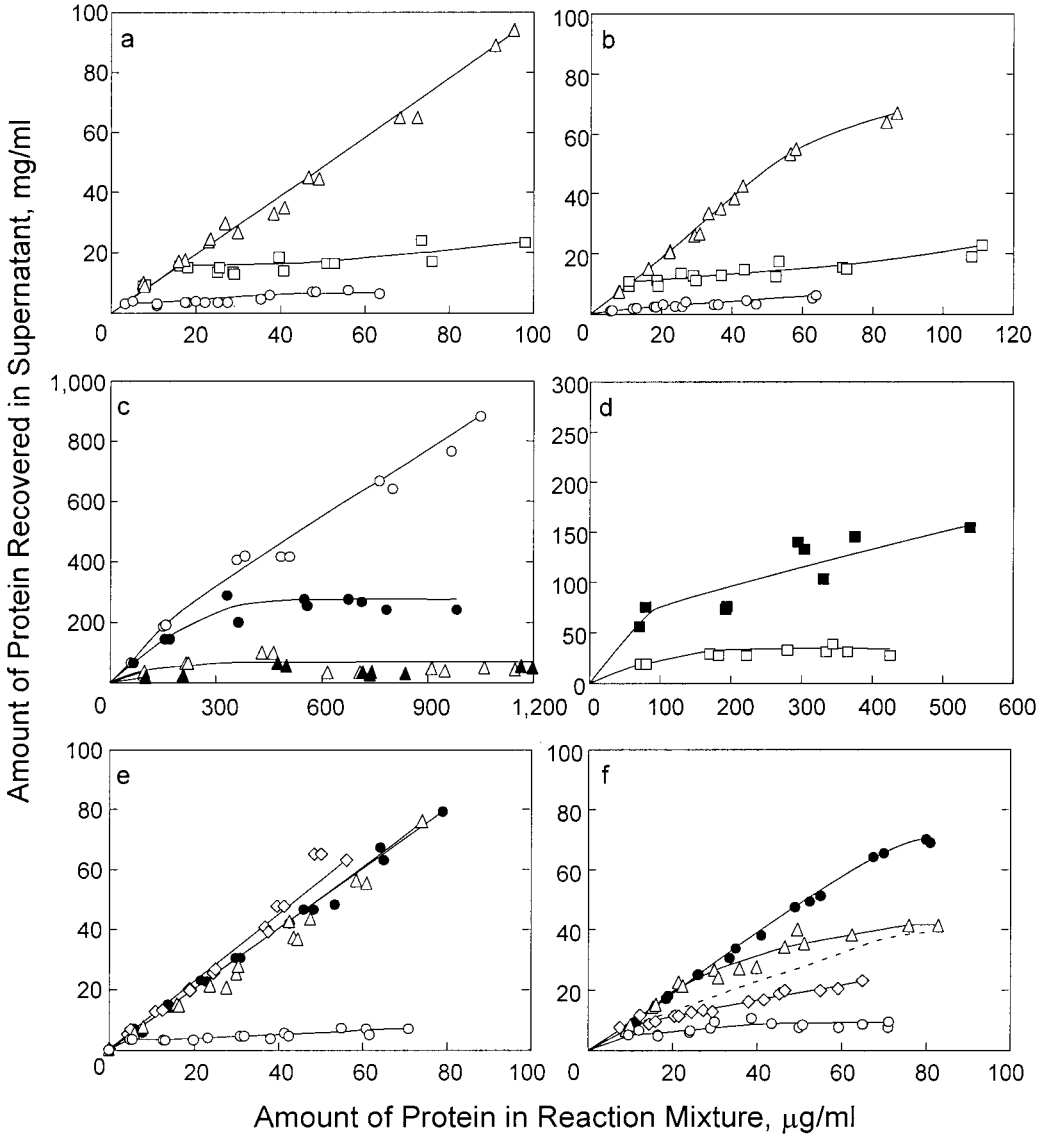

FIGURE 2: Assembly properties of MIIB$^{\alpha F47}$ and its mutants at various protein concentrations. Various amounts of fragments were incubated in the presence of 0.15 M NaCl with or without Mg^{2+}. Amounts of protein recovered in the supernatant are shown. Assembly of MIIB$^{\alpha F47}$ and its mutants without (a) or with (b) Mg^{2+}: (○) MIIB$^{\alpha F47}$-wt, (△) MIIB$^{\alpha F47}$-CK-5D, and (□) MIIB$^{\alpha F47}$-PK-2D. (c) Assembly studies using higher protein concentrations: (○ and ●) MIIB$^{\alpha F47}$-CK-5D, (△ and ▲) MIIB$^{\alpha F47}$-PK-2D, (white symbols) without Mg^{2+}, and (black symbols) with Mg^{2+}. (d) Assembly of MIIB$^{\alpha F47}$-PK-4D alone or mixed with MIIB$^{\alpha F47}$-wt in the presence of Mg^{2+}: (■) MIIB$^{\alpha F47}$-PK-4D and (□) homofragment mixtures of MIIB$^{\alpha F47}$-PK-4D with MIIB$^{\alpha F47}$-wt (1:1 ratio). Assembly of MIIB$^{\alpha F47}$-wt and its CK-5D mutants without (e) and with (f) Mg^{2+}. Equal amounts of MIIB$^{\alpha F47}$-wt and MIIB$^{\alpha F47}$-CK-5D were mixed in the presence of 6 M urea at room temperature for 30 min, dialyzed at 4 °C against a buffer containing 10 mM imidazole-HCl (pH 7.5), 0.6 M NaCl, and 1 mM EDTA, and then microcentrifuged for 30 min. The resultant supernatants, regarded as W/CK-D heterofragments, contain theoretically a mixture of homofragments and heterofragments of W_2, W/CK-D, and CK-D_2 in a 1:2:1 ratio. Equal amounts of MIIB$^{\alpha F47}$-wt and CK-5D mutants also were mixed in the absence of urea (homofragment mixture, W_2 + CK-D_2). The dotted line (f) represents the average values of MIIB$^{\alpha F47}$-wt alone and MIIB$^{\alpha F47}$-CK-5D alone: (○) MIIB$^{\alpha F47}$-wt, (●) MIIB$^{\alpha F47}$-CK-5D, (△) W/CK-D heterofragments, and (◇) homofragment mixtures (W_2 + CK-D_2).

The average recovery values of MIIB$^{\alpha F47}$-wt and -CK-5D were calculated to illustrate an expected line if wt and the CK-5D mutant assemble independently (dotted line, Figure 2f). The homofragment mixtures, W_2 + CK-D_2, assembled at protein concentrations of >20 μg/mL, and their recovery rates were clearly lower than the dotted line at protein concentrations of >30 μg/mL. Thus, MIIB$^{\alpha F47}$-wt as homofragments appeared to enhance the assembly of MIIB$^{\alpha F47}$-CK-5D homofragments. However, within the concentration range of W_2 + CK-D_2 that was used, the amounts of proteins remaining in the supernatant apparently did not reach a plateau level. The W/CK-D started to assemble at concentrations of >30 μg/mL (0.32 μM fragments). Their recovery patterns were clearly above the dotted line, indicating that MIIB$^{\alpha F47}$-CK-5D in heterofragments reduced the assembly property of MIIB$^{\alpha F47}$-wt.

Similarly, the critical concentration for MIIB$^{\alpha F47}$-PK-4D assembly was lowered by mixing with an equal amount of MIIB$^{\alpha F47}$-wt in the presence of Mg^{2+} (Figure 2d); the value for the homofragment mixture (W_2 + PK-D_2) was estimated to be around 25 μg/mL (0.27 μM fragments). If MIIB$^{\alpha F47}$-wt did not coassemble with MIIB$^{\alpha F47}$-PK-4D, the supernatant concentration of the mixture would be around 70−80 μg/mL (the average of MIIB$^{\alpha F47}$-wt and PK-4D under similar

Table 2: Summary of Critical Concentrations for Assembly of MIIB$^{\alpha F47}$ Containing Mutations at PK C and CK II Sites

MIIB$^{\alpha F47}$	[EDTA] (μg/mL)	[$MgCl_2$] (μg/mL)
wild type	3.0 ± 1.4	2.3 ± 1.9
PK-5A	2	3
PK-2D	21.7 ± 7.5	16.7 ± 7.6
PK-2E	22	18
PK-3E	90	50
PK-4D	≥300	150
W_2 + PK-D_2	>200	25
CK-5D	>1000	250
CK-5A	<1	<1
W/CK-D	>80	36.0 ± 4.0
W_2 + CK-D_2	>80	21.5 ± 1.5

conditions). Without Mg^{2+}, the homofragment mixture (W_2 + PK-D_2) did not sediment at all (not shown). This indicates that all of the MIIB$^{\alpha F47}$-wt should have formed heterodimers with the mutants independently of Mg^{2+} (thus, no filament was formed). The results depicted in Figure 2 suggest that the inhibition of MIIB$^{\alpha F47}$ assembly by PK C- or CK II-mediated phosphorylation is due to the increases in critical concentrations for assembly and that the phosphorylated and unphosphorylated MIIBs influence each other's assembly properties.

Coassembly of MIIA and MIIB in Vitro. Although phosphorylation of heavy chains by PK C and CK II inhibits assembly of MIIB$^{\alpha F47}$ in a system containing only MIIB$^{\alpha F47}$ (*9*), whether phosphorylation can prevent coassembly of MIIB with MIIA has not been addressed. To test this hypothesis, we analyzed the assembly properties of MIIB$^{\alpha F47}$-wt, -PK-4D, and -CK-5D in the presence of MIIA^{F46}. MIIA^{F46} and MIIB$^{\alpha F47}$ have distinct sensitivities to salt concentrations for their assembly, especially in the presence of Mg^{2+} (*9*). As seen in panels a and b of Figure 3, more MIIA^{F46} than MIIB$^{\alpha F47}$-wt was recovered in the supernatants between 0.15 and 0.2 M NaCl. The recoveries of pure MIIA^{F46} and MIIB$^{\alpha F47}$-wt at 0.175 M NaCl were calculated as 55 and 15%, respectively. When mixing with MIIA^{F46} was carried out, the percent recovery of MIIB$^{\alpha F47}$-wt clearly increased at NaCl concentrations between 150 and 200 mM, and the ratios of MIIA^{F46} to MIIB$^{\alpha F47}$ became almost equal (Figure 3b, lower panel). This suggests that MIIA^{F46} and MIIB$^{\alpha F47}$-wt coassembled. Approximately 50−60, 80−90, and 90−100% of MIIB$^{\alpha F47}$-CK-5D were recovered in the supernatants at 0.125, 0.15, and 0.175 M NaCl, respectively (Figures 1 and 3c, upper panel). When mixing with MIIA^{F46} was carried out, the amounts of MIIB$^{\alpha F47}$-CK-5D recovered in the supernatants clearly decreased between 0.1 and 0.175 M NaCl (Figure 3c, lower panel). In addition, the amounts of MIIA^{F46} recovered in the supernatants from the mixtures with MIIB$^{\alpha F47}$-CK-5D appeared to be greater than those with MIIB$^{\alpha F47}$-wt. In the presence of 2.5 mM Mg^{2+}, 60% of the MIIB$^{\alpha F47}$-PK-4D remained in the supernatants at 0.15 M NaCl, and practically all of the fragments were recovered at >0.175 M (Figure 3d upper panel, e). When MIIB$^{\alpha F47}$-PK-4D was mixed with MIIA^{F46}, the recovery patterns of MIIB$^{\alpha F47}$-PK-4D were dissimilar to those of MIIA^{F46} at salt concentrations of ≤0.175 M (Figure 3d, lower panel). The relative recovery rates of MIIA^{F46} and MIIB$^{\alpha F47}$-PK-4D were measured by running a separate set of gels under conditions that allowed improved separation of the two isoform bands. Percent recoveries for each isoform in

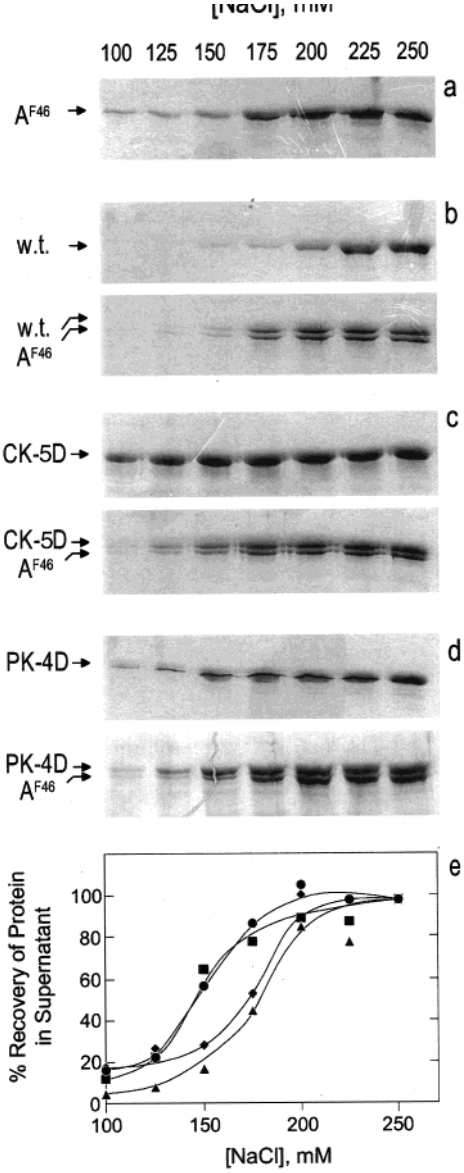

FIGURE 3: Changes in assembly rates by mixing MIIA^{F46} with MIIB$^{\alpha F47}$. MIIA^{F46} and MIIB$^{\alpha F47}$ (-wt, -PK-4D, or -CK-5D) were mixed in an equal ratio in buffer C. Filament assembly of the mixtures was tested in the presence of 2.5 mM Mg^{2+} and various NaCl concentrations as described in the legend of Figure 1. Supernatants were subjected to 12.5% SDS−PAGE (*26*) followed by Coomassie blue staining. For each lane, 25 μL of the samples was applied. The final NaCl concentrations are shown in millimolar at the top of panel a: (a) MIIA^{F46} alone, (b) MIIB$^{\alpha F47}$-wt with or without MIIA^{F46}, (c) MIIB$^{\alpha F47}$-CK-5D with or without MIIA^{F46}, and (d) MIIB^{F47}-PK-4D with or without MIIA^{F46}. (e) Relative amounts of MIIA^{F46} and MIIB$^{\alpha F47}$-PK-4D recovered in the supernatants for the samples used in panel d. For panel e, the samples used in d were reapplied to SDS−PAGE with a lower current and for a longer time than in panels a−d for better separation of the two closely migrating bands until the prestained ovalbumin band reached the middle of the gels. After Coomassie blue staining and destaining, each protein band was cut out, and the amounts of the dye bound to the bands were measured as described in ref *27*. Areas without any protein from corresponding gels were used to determine background, the value of which was subtracted from each sample. Percent recoveries of MIIA^{F46} and MIIB$^{\alpha F47}$-PK-4D at various salt concentrations were calculated, for each gel, by taking the amounts of dye bound to each isoform band at 0.25 M NaCl as 100%. The values are an average of the two independent runs: (◆) MIIA^{F46}, (■) MIIB^{F47}-PK-4D, (▲) MIIA^{F46} recovered from mixtures of MIIA^{F46} and MIIB^{F47}-PK-4D, and (●) MIIB^{F47}-PK-4D recovered from mixtures of MIIA^{F46} and MIIB^{F47}-PK-4D.

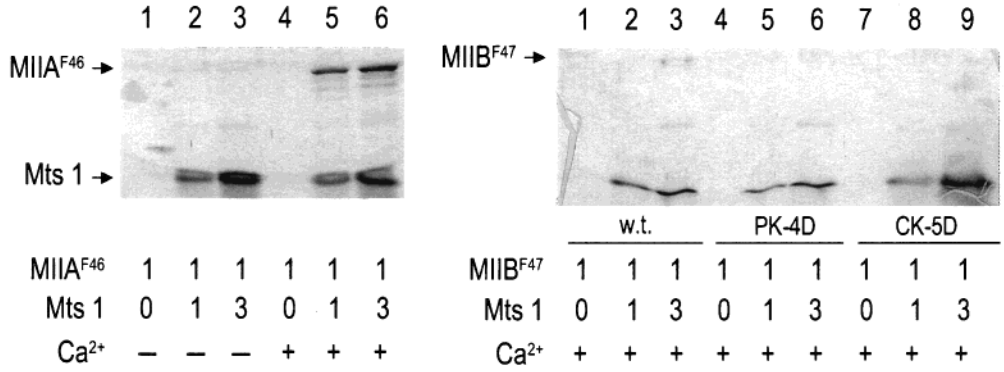

FIGURE 4: Binding of mts 1 to MIIA^{F46} and MIIB$^{\alpha F47}$. Binding of mts 1 to MIIA^{F46} (left panel) or MIIB$^{\alpha F47}$ (right panel) was tested with or without Ca^{2+} as described in Materials and Methods. The proteins eluted from the Ni−NTA resin were subjected to 12.5% SDS−PAGE (*25*). The molar ratios of mts 1 to the heavy chain peptide with or without Ca^{2+} are shown in the figure. After boiling, 25 μL of the samples was applied for each lane. The differences in the staining intensities of mts 1 in the two panels for corresponding lanes were likely due to the differences in running conditions between two gels.

the supernatants (Figure 3e) revealed that the assembly rates of MIIB$^{\alpha F47}$-PK-4D were unchanged by addition of MIIA^{F46} at various salt concentrations. Similarly, the assembly rates of MIIA^{F46} did not change with and without MIIB$^{\alpha F47}$-PK-4D, indicating that in the presence of 2.5 mM Mg^{2+}, MIIA^{F46} and MIIB$^{\alpha F47}$-PK-4D may not form heterofilaments.

Specific Binding of Mts 1 to MIIA. Mts 1 is reported to bind to both MIIA and MIIB at the rod region (*22*) or to inhibit PK C-mediated phosphorylation of MIIA by binding to the tail end (*23*). Although the sequence around a single PK C site found in MIIA (*15*, *16*) is well-conserved in MIIB (Figure 1 in ref 9 for a summary of amino acid sequences), major PK C sites in MIIB are at locations specific to MIIB. To test the specificity of binding of mts 1 to nonmuscle myosins, MIIA^{F46} and MIIB$^{\alpha F47}$ were incubated with mts 1 having a polyhistidine tag at its N-terminus, in the presence of 0.2 M NaCl to prevent assembly of the fragments. Both mts 1 and its complexes with heavy chains were recovered by Ni−NTA affinity resins. The proteins eluted from the resins were analyzed by SDS−PAGE (*25*), permitting separation of low-molecular weight mts 1 from heavy chain fragments. As shown in Figure 4 (left panel), MIIA^{F46} did not bind to the Ni−NTA resins in the absence of either mts 1 (lanes 1 and 4) or Ca^{2+} (lanes 2 and 3). MIIA^{F46} bound to the resins only when both mts 1 and Ca^{2+} were added, and the amounts of bound MIIA^{F46} increased when the ratio of mts 1 to MIIA^{F46} was increased (lanes 5 and 6). Under the same conditions, only trace amounts of MIIB$^{\alpha F47}$-wt bound to the Ni−NTA resins at a higher molar ratio of mts 1 (Figure 4, right panel, lane 3). No detectable levels of MIIB$^{\alpha F47}$ were recovered from the resin when the PK-4D and CK-5D mutants were used (right panel, lanes 4−9). These results suggest that phosphorylation of MIIB by PK C or CK II will not increase the extent of interaction of MIIB with mts 1 and that the mts 1 binds rather specifically to MIIA.

Inhibition of MIIA Assembly by Mts 1. The mts 1−heavy chain binding also was tested by mixing the components in the presence of 0.6 M NaCl followed by reducing the salt concentrations to 0.1, 0.15, or 0.2 M. After ultracentrifugation, the amounts of the heavy chain fragments and mts 1 recovered in the supernatants were analyzed by SDS−PAGE (*25*). At a final NaCl concentration of 0.1 M, only trace amounts of MIIA^{F46} were recovered in the supernatants for

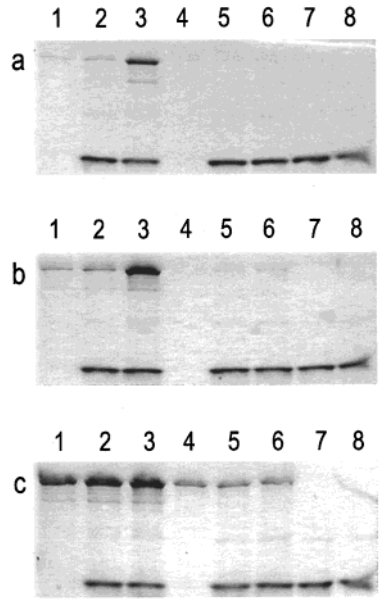

FIGURE 5: Inhibition of MIIA^{F46} assembly by mts 1. Monomeric MIIA^{F46} or MIIB$^{\alpha F47}$ in buffer C was mixed with or without Ca^{2+} and mts 1 (3:1 molar ratio of mts 1 to heavy chain peptide). The final NaCl concentrations were adjusted to 0.1 (a), 0.15 (b), or 0.2 M (c) by adding buffer B and 1 M NaCl as described in Materials and Methods. Mg^{2+} was added to a concentration of 2.5 mM at the last step. After ultracentrifugation, the supernatant fractions were subjected to SDS−PAGE (*25*) as described in the legend of Figure 4: lanes 1 and 4, heavy chain only; lanes 2 and 5, heavy chain with mts 1, without Ca^{2+}; lanes 3 and 6, heavy chain, mts 1, and Ca^{2+}; lane 7, mts 1; lane 8, mts 1 and Ca^{2+}; lanes 1−3, MIIA^{F46}; lanes 4−6, MIIB$^{\alpha F47}$-wt.

the samples containing MIIA^{F46} alone or MIIA^{F46} with mts 1 but no Ca^{2+} (Figure 5a, lanes 1 and 2). When both mts 1 and Ca^{2+} were added, a significant amount of MIIA^{F46} was recovered in the supernatants (Figure 5a, lane 3). When the salt concentrations were increased to 0.15 M, more MIIA^{F46} was recovered in the supernatant in the presence of both Ca^{2+} and mts 1 (Figure 5b, lane 3). Without mts 1 or Ca^{2+}, the recovery rates increased only slightly (Figure 5b, lanes 1 and 2). At 0.2 M NaCl, practically all of the MIIA^{F46} was found in the supernatants for all samples (Figure 5c, lanes 1−3). In contrast, almost all of the MIIB$^{\alpha F47}$-wt was sedimented by ultracentrifugation until the salt concentrations increased to 0.2 M, and there was no difference in the recovery rates of MIIB$^{\alpha F47}$ with or without Ca^{2+}-mts 1

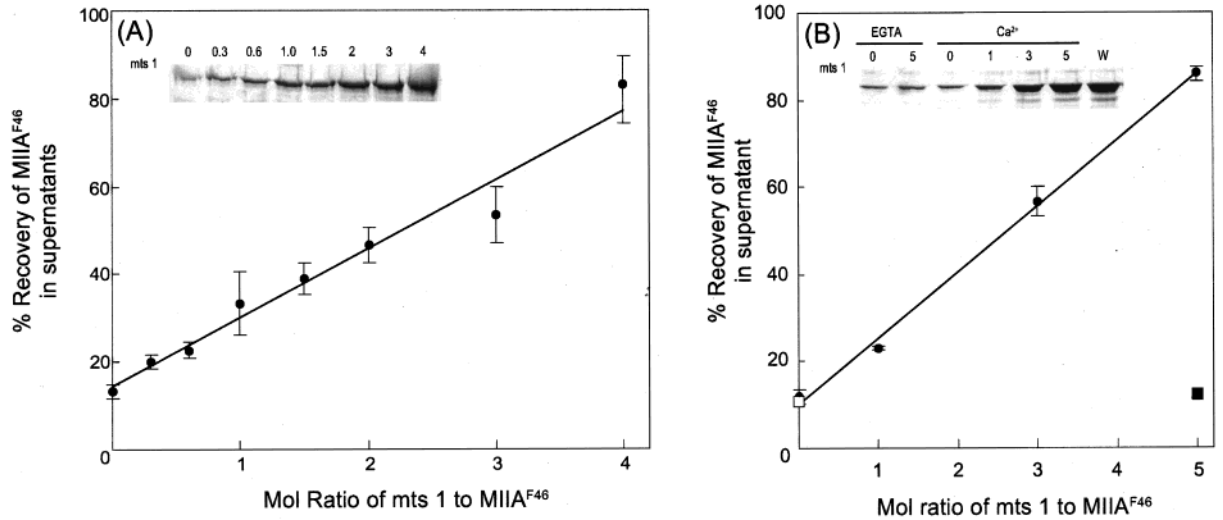

FIGURE 6: (A) Inhibition of MIIA^{F46} assembly by mts 1 at various molar ratios. Monomeric MIIA^{F46} (30 μg) was mixed with mts 1 at various molar ratios (0−4:1 mts 1 to MIIA^{F46}) in the presence of Ca^{2+}. Final concentrations of NaCl, Ca^{2+}, and Mg^{2+} were adjusted to 0.15 M, 0.1 mM, and 2.5 mM, respectively, in a final volume of 0.15 mL as described in the legend of Figure 5. (B) Dissociation of MIIA^{F46} filaments by mts 1 at various molar ratios. MIIA^{F46} filaments (30 μg) prepared with either 0.1 mM Ca^{2+} or 0.1 mM EGTA as described for panel A were incubated at 4 °C for 1 h with mts 1 at various molar ratios, in a final volume of 0.15 mL: (●) mts 1 with Ca^{2+}, (□) without mts 1-Ca^{2+}, (■) mts 1 and MIIA^{F46} in a 5:1 ratio with EGTA, and (W) whole reaction mixture. For panels A and B, the amounts of MIIA^{F46} recovered in the supernatants were measured as described in the legend of Figure 3e. Percent recoveries of MIIA^{F46} were calculated by taking the amounts of the dye bound to MIIA^{F46}, for each sample, before centrifugation, as 100%. Data represent an average of four (A) and three (B) independent measurements. The insers in panels A and B are the representative gels after Coomassie blue staining, where molar ratios of mts 1 to MIIA^{F46} are shown at the top of the figures.

(Figure 5a−c, lanes 4−6). These results suggest that mts 1 specifically binds to MIIA and inhibits its assembly and that the extent of the inhibition depends on the salt concentrations.

The inhibition profile was determined by measuring the amounts of MIIA^{F46} in the supernatants after ultracentrifugation, at various molar ratios of mts 1 to MIIA^{F46} (Figure 6A). The percent recovery of MIIA^{F46} increased proportionally to the amounts of mts 1 added. Extrapolation of the line in Figure 6A indicates that mts 1 in a molar ratio of 5:1 is required for 100% inhibition of MIIA^{F46} assembly at pH 7.5 in the presence of 0.15 M NaCl, 2.5 mM Mg^{2+}, and 0.1 mM Ca^{2+}. Judging from the ultracentrifugation conditions used here, the MIIA bound to mts 1 is likely monomeric.

A further study was carried out to test whether mts 1 could selectively inhibit MIIA assembly in the mixtures of MIIA and MIIB. For this, premixed MIIA^{F46} and MIIB$^{\alpha F47}$ in 0.6 M NaCl were incubated in the presence of Ca^{2+} with or without mts 1; then, the final salt concentration was adjusted to 0.15 M. The proteins recovered in the supernatants and precipitates were analyzed by SDS−PAGE (*25*) (Figure 7a,b). Consistent with the results shown in Figures 5 and 6A, Ca^{2+}-mts 1 strongly inhibited the assembly of MIIA^{F46} (Figure 7a,b, lanes 2), but did not affect that of MIIB$^{\alpha F47}$ (lanes 6). Most of MIIA^{F46} and MIIB$^{\alpha F47}$ in the mixtures sedimented when mts 1 was omitted (Figure 7a,b, lanes 3), whereas the amounts of proteins in the supernatants were increased by including mts 1 (lane 4 in Figure 7a). A small fraction of mts 1 sedimented only when the heavy chain fragments (MIIA^{F46} and/or MIIB$^{\alpha F47}$) were present (Figure 7b, lanes 2, 4, and 6). Via application of the samples to SDS−PAGE with a Tris-glycine buffer (*26*), it became clear that, when both mts 1 and Ca^{2+} were added to the mixtures, most of the isoform recovered in the supernatant was MIIA^{F46} (Figure 7c, lane 4), whereas the one that sedimented was exclusively MIIB$^{\alpha F47}$ (Figure 7d, lane 4). Without mts 1, most

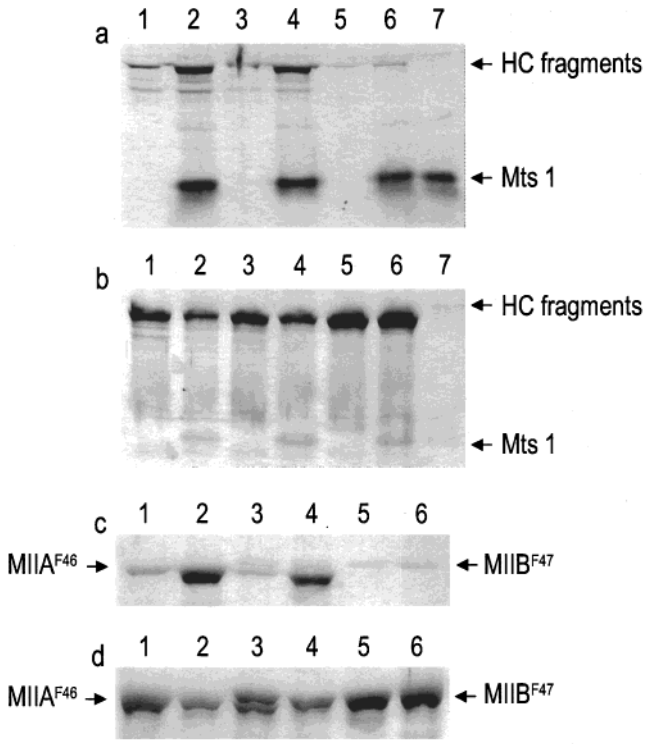

FIGURE 7: Selective inhibition of MIIA^{F46} assembly by mts 1 in MIIA and MIIB mixtures. MIIA^{F46} and MIIB$^{\alpha F47}$ were premixed in the presence of Ca^{2+} with or without mts 1. The final NaCl, Ca^{2+}, and Mg^{2+} concentrations were the same as described in the legend of Figure 6A. After ultracentrifugation, the supernatants were subjected to SDS−PAGE with a Tris-tricine (a and b) or Tris-glycine (c and d) buffer: (a and c) supernatants; (b and d) precipitates; lane 1, MIIA^{F46}; lane 2, MIIA^{F46} and mts 1; lane 3, MIIA^{F46} and MIIB$^{\alpha F47}$; lane 4, MIIA^{F46}, MIIB$^{\alpha F47}$, and mts 1; lane 5, MIIB$^{\alpha F47}$; lane 6, MIIB$^{\alpha F47}$ and mts 1; and lane 7, mts 1 only.

of the MIIA^{F46} and MIIB$^{\alpha F47}$ sedimented (Figure 7c,d, lanes 3). These results show that mts 1 is a protein that selectively

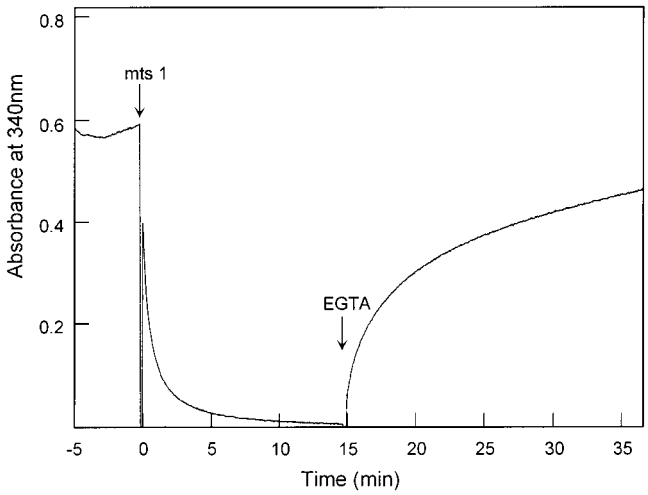

FIGURE 8: Ca^{2+}-dependent effect of mts 1 on $MIIA^{F46}$ filaments: changes in turbidity at 340 nm. $MIIA^{F46}$ filaments (60 μg/0.4 mL) prepared as described in the legend of Figure 6A were transferred into a cuvette (2 mm width), and the turbidity at 340 nm was recorded at room temperature. At time 0, mts 1 (65 μg) at a 5:1 molar ratio (mts 1 to $MIIA^{F46}$ peptide) was added into the cuvette. When the absorbance at 340 nm decreased to a basal level (at 15 min), EGTA was added to the cuvette at a final concentration of 0.2 mM.

binds to MIIA and inhibits its assembly in a Ca^{2+}-dependent manner without affecting the $MIIB^{\alpha F47}$.

Disassembly of $MIIA^{F46}$ Filaments by Mts 1. The effect of mts 1 on the stability of the $MIIA^{F46}$ filament was also tested at 0.05 and 0.15 M NaCl by using various molar ratios of mts 1 with or without Ca^{2+}. In the presence of 0.05 M NaCl, 2.5 mM Mg^{2+}, and 0.1 mM Ca^{2+} at pH 7.5, no detectable levels of $MIIA^{F46}$ were found in the supernatant with the method that was used. Addition of mts 1 only slightly disassembled the filaments at a molar ratio of 5:1 to $MIIA^{F46}$; the amounts of $MIIA^{F46}$ in the supernatants increased to 5% of the total $MIIA^{F46}$ added. In contrast, at 0.15 M NaCl, the amounts of $MIIA^{F46}$ recovered in the supernatants increased linearly with mts 1 concentration (Figure 6B); nearly 90% of the preformed $MIIA^{F46}$ filaments were dissociated by mts 1 at a molar ratio of 5:1 to $MIIA^{F46}$. Again, mts 1 had no effect on the filaments when Ca^{2+} was omitted from the reaction mixtures.

Disassembly of $MIIA^{F46}$ filaments by mts 1 was monitored by measuring the turbidity at 340 nm in the presence of 0.15 M NaCl (Figure 8). When mts 1 was added to the $MIIA^{F46}$ filaments at a 5:1 molar ratio, the absorbance at 340 nm rapidly declined; the reading decreased from 0.6 to 0.3 in less than 30 s, and reached equilibrium by 5 min. The result from Figure 6B indicates that this decrease in turbidity is due to dissociation of $MIIA^{F46}$ filaments into monomers. When Ca^{2+} was chelated out by addition of EGTA, the reading at 340 nm quickly increased, indicating reassembly of $MIIA^{F46}$ filaments. These results depicted in Figures 6B and 8 show that mts 1 not only inhibits $MIIA^{F46}$ filament formation but also dissociates the filaments in a Ca^{2+}-dependent manner and that the effects of mts 1 are rapid and reversible.

DISCUSSION

We have shown two independent mechanisms for regulating MIIA and MIIB assembly via the tail-end region. The mechanisms involve mts 1 binding to MIIA and phosphorylation of MIIB. Mts 1 functioned to keep $MIIA^{F46}$ in monomers by inhibiting the assembly as well as by dissociating the pre-existed filaments. Mutation to Asp at the PK C and CK II sites inhibited MIIB assembly by significantly increasing the critical concentrations. Mg^{2+} and unphosphorylated MIIB influenced the critical concentrations. Homofilaments of MIIA and MIIB could be formed by selectively inhibiting the assembly of MIIB and MIIA, respectively.

Mutation and the Critical Protein Concentrations for MIIB Assembly. Mutation of $MIIB^{\alpha F47}$ to Asp at five CK II sites inhibited the fragment assembly, and the salt-dependent assembly pattern resembled that of $MIIB^{\alpha F47}$ phosphorylated by CK II. Mutation to either Asp or Glu at two proximal locations (at major PK C sites, PK-2D or -2E) of five potential PK C sites noticeably increased the critical concentrations for $MIIB^{\alpha F47}$ assembly. However, both types of mutation did not fully mimic the PK C-mediated effect. There could be three possibilities for this. (I) The two negative charges created by two COO^- groups are not equivalent to PO_4^{2-}. In the case of smooth muscle myosin, when the regulatory light chains are mutated to either Glu or Asp at two adjacent residues (Thr-18 and Ser-19), the mutations mimic the effect of the myosin light chain kinase-mediated phosphorylation on myosin conformation. However, such mutations have a minor effect on activation of the actin-activated myosin ATPase activity or F-actin sliding motility (*28*). For $MIIB^{\alpha F47}$ assembly, increases in the critical concentrations were observed by increasing the number of acidic amino acids that were replaced. In the case of *Dictyostelium* myosin, mutation at three phosphorylation sites to Asp mimics the effect of phosphorylation on assembly (*29*). Clearly, this was not the case for $MIIB^{\alpha F47}$; assembly patterns of the $MIIB^{\alpha F47}$ phosphorylated by PK C resembled those of PK-4D, in the presence of various salt concentrations. (II) Since the PK-C sites are within a basic environment, if a site in one peptide is phosphorylated, the equivalent site in the other peptide would no longer be phosphorylatable. Instead, one distal position among the other four sites could be recognized by the kinase. If this is the case, mutation at two sites at different positions between two heavy chains (total four distinct sites as a dimer) might cause inhibition similar to the MIIB assembly as PK-4D. (III) Alternatively, it was also possible that the Ala replaced in PK-2D/2E reduced the effects of two carboxylate groups.

The function of the tailpiece for smooth muscle and nonmuscle myosins II is suggested to enhance assembly rather than to be absolutely required for assembly. In the case of MIIA (chicken brush border myosin II), deletion of 35 amino acids from the COOH terminus increased the critical concentration for myosin rod assembly by 50-fold (*14*). This study showed that inhibition of MIIB assembly by the Asp/Glu mutation at the PK C or CK II sites was also due to the significant increases in critical concentrations. We speculate that acidification would cause (1) repulsion of two heavy chains at the tail-end domains (CK II sites), (2) a conformational change at the junction between the helical rod and the nonhelical tail-end domain, which separates the tail-end domain from the rod backbone (PK C sites) of MIIB, or (3) weakening of intermolecular electrostatic interactions of the tail-end domain with the rod. Such

changes would shift the equilibrium from monomers to filaments. Phosphorylation of MIIB by the kinases probably does the same.

Mg $^{2+}$ Effects on MIIB Assembly. We observed three distinct effects of Mg^{2+} on MIIB$^{\alpha F47}$ assembly. (1) At low salt concentrations, Mg $^{2+}$ enhanced the assembly of all types of MIIB$^{\alpha F47}$ mutants (except for MIIB$^{\alpha F47}$-CK-5A). At low salt concentrations, Mg^{2+} induced *Acanthamoeba* myosins to form lateral aggregations of minifilaments but not to assemble monomers or intermediates into minifilaments (*30*, *31*). In a similar manner, Mg^{2+} might enhance the assembly of MIIB$^{\alpha F47}$ (and its mutants). (2) At physiological salt concentrations, Mg^{2+} significantly decreased the critical concentrations for assembly of the Asp/Glu mutants. (3) At 0.15 M NaCl, Mg^{2+} also enhanced coassembly of MIIB$^{\alpha F47}$-wt and MIIB$^{\alpha F47}$-CK-5D (and with MIIB$^{\alpha F47}$-PK-4D) in mixtures of both heterofragments and homofragments. Under physiological ionic strength, Mg^{2+} must affect the conformation of the tail-end domain or a junction between the α-helical rod and nonhelical tail-end domain of each mutant. Alternatively, it strengthens the electrostatic interactions at pH 7.5 among the mutants by reducing the negative charges at the tail end.

Homofilament Formation by MIIB Phosphorylation. MIIB$^{\alpha F47}$-wt coassembled with MIIA^{F46} in a wide range of salt concentrations. In contrast to one's expectation, MIIB$^{\alpha F47}$-CK-5D also coassembled with MIIA^{F46}. However, because the amounts of MIIB$^{\alpha F47}$-CK-5D and MIIA^{F46} recovered in the supernatants were somewhat larger than those of MIIB$^{\alpha F47}$-wt and MIIA^{F46}, the CK II-mediated phosphorylation of MIIB might reduce the overall rates of assembly of MIIB−MIIA heteromers into large filaments. Mg^{2+} made the assembly of MIIA^{F46} more sensitive to salt concentrations as reported previously (*9*), but enhanced that of MIIB$^{\alpha F47}$-PK-4D (Figure 4); thus, Mg^{2+} made the differences in assembly between MIIA^{F46} and MIIB$^{\alpha F47}$-PK-4D (in a homogeneous system) smaller in a wide range of salt concentrations. Despite this, a close examination of the recovery patterns revealed that MIIA^{F46} and MIIB$^{\alpha F47}$ did not form heterofilaments when MIIB$^{\alpha F47}$-PK-4D was used. Thus, phosphorylation of MIIB by PK C appears to function also to prevent formation of heterofilaments between MIIA and MIIB.

Mts 1 and MIIA Assembly. A relatively large amount of mts 1 is expressed in highly metastatic cells and also in highly motile normal cells such as activated macrophages, T-lymphocytes, and neutrophils, as well as in tissues such as thymus, spleen, and bone marrow (*18*, *19*, *32*, *33*). However, immunocytochemical studies have revealed that this protein is expressed in most normal adult tissues (*17*). In contrast to those of Ford et al. (*22*), our results strongly suggest that mts 1 is the protein which binds specifically to MIIA^{F46}. The mts 1 binding caused both inhibition of MIIA assembly and disassembly of the preformed MIIA filaments. Moreover, mts 1 selectively inhibited MIIA^{F46} assembly in the MIIA^{F46} and MIIB$^{\alpha F47}$ mixtures without affecting that of MIIB$^{\alpha F47}$. Some levels of mts 1, however, bound to the filaments of MIIA^{F46} as well as MIIB$^{\alpha F47}$ (Figure 7b). This could explain the discrepancies between our results and those of Ford et al. (*22*); in their study, the assay was carried out at a low salt concentration, in which most of MIIB should form filaments. Mts 1 may bind to MIIB with a significantly low affinity. The binding, however, may not have physiological importance on the MIIB filaments. Kriajevska et al. (*23*) mapped the binding site for mts 1 to the tail end of MIIA. Our results support their conclusion; on the basis of the binding specificity and the isoform specific amino acid sequences (*1*, *34*, *35*), the major mts 1 binding site in MIIA must be within the nonhelical tail-end domain. During proteolytic preparation of rods from the intact myosins, nonhelical tail-end domains are highly likely to be truncated (*9*); thus, it is not surprising that mts 1 had no effect on myosin rods generated by papain digestion of platelet myosin II (*22*).

Physiological Significance. In vivo phosphorylation of the MIIA isoform is known in human platelets (*36*), macrophages (*37*), rat basophilic leukemia cells (RBL) (*38*) (all express MIIA only), and *Xenopus* oocytes (*39*). Among them, PK C is a kinase responsible for phosphorylation of MIIA in platelets and RBL cells. In contrast, there is no definitive work on in vivo phosphorylation of MIIB by PK C or CK II. In *Xenopus* XTC cells or oocytes, cyclin-p34^{cdc2} kinase phosphorylates MIIB both in vivo and in vitro at the peptide-inserted region within the myosin head (*39*). In that study, Kelley et al. also described MIIB phosphorylation both in vivo and in vitro by kinase(s) other than cyclin-p34^{cdc2} kinase, yet they did not identify the kinase(s). These *Xenopus* cells express MIIA as a major isoform while MIIB is minor, and the extent of phosphorylation within MIIB was far greater than within MIIA. On the bases of our previous studies using MIIA^{F46} and MIIB$^{\alpha F47}$, MIIB has greater potential to be phosphorylated by both PK C and CK II than MIIA. Because the MIIA isoform is phosphorylated stoichiometrically by PK C in vivo (*36*, *38*) and because PK C and CK II are ubiquitously expressed kinases, it is reasonable to believe that MIIB can also be phosphorylated in vivo by both kinases in cells. Nonmuscle myosin concentrations are assumed to be within the range of 0.02−2 μM from erythrocytes to platelets (*40*). If it is assumed that critical concentrations of phosphorylated MIIB$^{\alpha}$ increase to levels similar to those of the Asp mutants, the cellular concentrations of nonmuscle myosins are apparently within the critical concentrations for assembly of phosphorylated MIIB$^{\alpha}$ (2.7 and 1.6 μM for MIIB$^{\alpha F47}$-CK-5D and -PK-4D, respectively). Local assembly of the phosphorylated MIIB can be seen when unphosphorylated MIIB coexists or the concentrations of phosphorylated MIIB increase significantly. MIIA may assist in assembly of the MIIB phosphorylated by CK II into filaments. However, MIIA homofilament assembly can be achieved by the PK C-mediated phosphorylation.

MIIA with higher enzymatic activity would generate greater cell movement in speed and force than MIIB. Constant assembly and disassembly of MIIA filaments, therefore, must be required for efficient movement of highly motile cells. It is not clear exactly how mts 1 promotes the invasiveness of highly metastatic cells. Mts 1 can function not only to maintain rapid turnover of MIIA filaments by disassembling filaments or by preventing assembly of MIIA (at when and where MIIA functions are not required) but also to prevent heterofilament formation between MIIA and MIIB. In addition, mts 1 binds to actin filaments and bundles them (*41*) and also binds to nonmuscle tropomyosin (*42*). Therefore, mts 1 can be a dual regulator for "actomyosin" machinery in cell movement. However, mts 1 requires

relatively high concentrations of Ca^{2+} for binding to the targets (*42*). Therefore, mts 1-mediated regulation of actomyosin could be seen only locally and momentarily when and where Ca^{2+} concentrations increased beyond the required levels. In conclusion, in cells expressing multiple nonmuscle myosin isoforms, homofilament assembly can be achieved via the tail-end region of myosins by two mechanisms: phosphorylation by PK C and CK II for MIIB and binding of mts 1 for MIIA.

ACKNOWLEDGMENT

We thank Dr. Marina Kriajevska for the generous gift of polyhistidine-tagged mts 1 expression vector and Drs. Marshall Elzinga and David Miller and Maureen Marlow for their critical reading of the paper. We acknowledge Sharon Mathier and Mary Ellen Cafaro for computer graphics.

REFERENCES

1. Saez, C. G., Myers, J. C., Shows, T. B., and Leinwand, L. A. (1990) *Proc. Natl. Acad. Sci. U.S.A. 87*, 1164−1168.
2. Simons, M., Wang, M., McBride, O. W., Kawamoto, S., Yamakawa, K., Gdula, D., Adelstein, R. S., and Weir, L. (1991) *Circ. Res. 69*, 530−539.
3. Cheng, T. P. O., Murakami, N., and Elzinga, M. (1992) *FEBS Lett. 311*, 91−94.
4. Maupin, P., Phillips, C. L., Adelstein, R. S., and Pollard, T. D. (1994) *J. Cell Sci. 107*, 3077−3090.
5. Kelley, C. A., Sellers, J. R., Gard, D. L., Bui, D., Adelstein, R. S., and Baines, I. C. (1996) *J. Cell Biol. 134*, 675−687.
6. Kolega, J. (1998) *J. Cell Sci. 111*, 2085−2095.
7. Pollard, T. D. (1975) *J. Cell Biol. 67*, 93−103.
8. Citi, S., Smith, R. C., and Kendrick-Jones, J. (1987) *J. Mol. Biol. 198*, 253−262.
9. Murakami, N., Chauhan, V. P. S., and Elzinga, M. (1998) *Biochemistry 37*, 1989−2003.
10. Taubman, M. B., Grant, J. W., and Nadal-Ginard, B. (1987) *J. Cell Biol. 104*, 1505−1513.
11. Grant, J. W., Taubman, M. B., Church, S. L., Johnson, R. L., and Nadal-Ginard, B. (1990) *J. Cell Biol. 111*, 1127−1135.
12. Cross, R. A., and Vanderkerckhove, J. (1986) *FEBS Lett. 200*, 355−360.
13. Ikebe, M., Hewett, T. E., Martin, A. F., Chen, M., and Hartshorne, D. J. (1991) *J. Biol. Chem. 266*, 7030−7036.
14. Hodge, T. P., Cross, R., and Kendrick-Jones, J. (1992) *J. Cell Biol. 118*, 1085−1095.
15. Conti, M. A., Sellers, J. R., Adelstein, R. S., and Elzinga, M. (1991) *Biochemistry 30*, 966−970.
16. Murakami, N., Elzinga, M., Singh, S. S., and Chauhan, V. P. S. (1994) *J. Biol. Chem. 269*, 16082−16090.
17. Gibbs, F. E. M., Barraclough, R., Platt-Higgins, A., Rudland, P. S., Wilkinson, M. C., and Parry, E. W. (1995) *J. Histochem. Cytochem. 43*, 169−180.
18. Ebralidze, A., Tulchinsky, E., Grigorian, M., Afanasyeva, A., Senin, V., Revazova, E., and Lukanidin, E. (1989) *Genes Dev. 3*, 1086−1093.
19. Grigorian, M., Tulchinsky, E., Burrone, O., Tarabykina, S., Georgiev, G., and Lukanidin, E. (1994) *Electrophoresis 15*, 463−468.
20. Davis, B. R., Davis, M. P. A., Gibbs, F. E. M., Barraclough, R., and Ruhmand, P. S. (1993) *Oncogene 8*, 999−1008.
21. Ford, H. L., Salim, M. M., Chakravarty, R., Aluiddin, V., and Zain, S. B. (1995) *Oncogene 11*, 2067−2075.
22. Ford, H. L., Silver, D. L., Kachar, B., Sellers, J. R., and Zain, S. B. (1997) *Biochemistry 36*, 16321−16327.
23. Kriajevska, M., Tarabykina, S., Bronstein, I., Maitland, N., Lomonosov, M., Hansen, K., Georgiev, G., and Lukanidin, E. (1998) *J. Biol. Chem. 273*, 9852−9856.
24. Lowry, O. H., Rosebrough, N. J., Farr, A. L., and Ransdall, R. J. (1951) *J. Biol. Chem. 193*, 265−275.
25. Schagger, H., and Jagow, G. (1987) *Anal. Biochem. 166*, 368−379.
26. Laemmli, U. K. (1970) *Nature 227*, 680−685.
27. Murakami, N., Singh, S. S., Chauhan, V. P. S., and Elzinga, M. (1995) *Biochemistry 34*, 16046−16055.
28. Sweeney, H. L., Yang, Z., Zhi, G., Stull, J. T., and Trybus, K. M. (1994) *Proc. Natl. Acad. Sci. U.S.A. 91*, 1490−1494.
29. Egelhoff, T. T., Lee, R. J., and Spudich, J. A. (1993) *Cell 75*, 363−371.
30. Sinard, J. H., and Pollard, T. D. (1989) *J. Cell Biol. 109*, 1529−1535.
31. Sinard, J. H., Rimm, D. L., and Pollard, T. D. (1990) *J. Cell Biol. 111*, 2417−2426.
32. Ford, H. L., and Zain, S. B. (1995) *Oncogene 10*, 1597−1605.
33. Jackson-Grusby, L. L., Swiergiel, J., and Linzer, D. I. H. (1987) *Nucleic Acids Res. 15*, 6677−6690.
34. Kuro-o, M., Nagai, R., Nakahata, K., Katoh, H., Tsai, R.-C., Tsuchimoto, H., Yasaki, Y., Ohkubo, A., and Takaku, F. (1991) *J. Biol. Chem. 266*, 3768−3773.
35. Phillips, C. L., Yamakawa, K., and Adelstein, R. S. (1995) *J. Muscle Res. Cell Motil. 16*, 379−389.
36. Kawamoto, S., Bengur, A. R., Sellers, J. R., and Adelstein, R. S. (1989) *J. Biol. Chem. 264*, 2258−2265.
37. Trotter, J. A., Nixon, C. S., and Johnson, M. A. (1985) *J. Biol. Chem. 260*, 14374−14378.
38. Ludowyke, R. I., Peleg, I., Braven, M. A., and Adelstein, R. S. (1989) *J. Biol. Chem. 264*, 12492−12501.
39. Kelley, C. A., Oberman, F., Yisraeli, J. K., and Adelstein, R. S. (1995) *J. Biol. Chem. 270*, 1395−1401.
40. Wong, A. J., Kiehart, D. P., and Pollard, T. D. (1985) *J. Biol. Chem. 260*, 46−49.
41. Watanabe, Y., Usada, N., Minami, H., Morita, T., Tsugane, S., Ichikawa, R., Kohama, K., Tomida, Y., and Hidaka, H. (1993) *FEBS Lett. 324*, 51−55.
42. Takenaga, K., Nakamura, Y., Sakiyama, S., Hasegawa, Y., Sato, K., and Endo, H. (1994) *J. Cell Biol. 124*, 757−768.

BI000347E